

Article

# The Contribution of Large Recurrent Sunspot Groups to Solar Activity: Empirical Evidence

Alexander Shapoval 

Faculty of Mathematics and Computer Science, University of Lodz, S. Banacha 22, 90-238 Łódź, Poland; alexander.shapoval@wmii.uni.lodz.pl

**Abstract:** We identify large sunspot nestlets (SN) mostly containing recurrent sunspot groups and investigate the indices of solar activity defined as the 11- or 22-year moving average of the daily areas of the SN. These nestlets, 667 in total, are constructed from the daily 1874–2020 RGO/SOON catalogue, which contains 41,394 groups according to their IDs, with a machine-learning technique. Within solar cycles 15–19, the index contributed disproportionately strongly to the overall solar activity: the index is normalized to a quasi-constant shape by a power function of the activity, where the exponent is approximately 1.35. Large SN contribute to solar activity even more in cycle 22, underlying the second largest peak of solar activity within the last Gleissberg cycle in ~1985. Introducing another composite, moderate SN normalized by the overall activity, we observe its quasi-constant shape in cycles 15–19 and a general anti-correlation with the first normalized composite. The constructed sunspot nestlets constitute a modified catalogue of solar activity. We define the average lifetime per day in 22-year windows for the modified catalogue, in line with Henwood et al. (SoPhys 262, 299, 2010), and reproduce the dynamics of this quantity they revealed for 1900–1965. The average lifetime derived from the moderate SN is found to form a wave with minima at the beginning of the 20th and 21st centuries, resembling the Gleissberg cycle with long minima. The average lifetime characterizing large SN exhibited a deeper minimum at the beginning of the 20th century than 100 years later.



**Citation:** Shapoval, A. The Contribution of Large Recurrent Sunspot Groups to Solar Activity: Empirical Evidence. *Universe* **2022**, *8*, 180. <https://doi.org/10.3390/universe8030180>

Academic Editors: Juha Kallunki and Arnold Hanslmeier

Received: 7 January 2022

Accepted: 4 March 2022

Published: 13 March 2022

**Publisher's Note:** MDPI stays neutral with regard to jurisdictional claims in published maps and institutional affiliations.



**Copyright:** © 2022 by the author. Licensee MDPI, Basel, Switzerland. This article is an open access article distributed under the terms and conditions of the Creative Commons Attribution (CC BY) license (<https://creativecommons.org/licenses/by/4.0/>).

**Keywords:** solar activity; long-lived sunspot groups; lifetime; Gleissberg cycle; machine learning

## 1. Introduction

The largest sunspots are characterized by a particular contribution to solar activity [1–6]. Identifying recurrent sunspot groups and adding their sizes to the statistical analysis, Nagovitsyn et al. [7] established that the coefficient of the proportionality in the Gnevyshev–Waldmeier rule is greater than earlier known estimates. The classification of sunspots into large, moderate, and small should ideally be universal going beyond the scope of individual papers. Obridko and Badalyan [2], splitting the range of sunspot areas into three intervals: up to 100 microhemispheres (MH), 100–500 MH, and >500 MH, found that the solar cycle “period” is most clearly detected with large sunspots, whereas the smaller sunspots somewhat unexpectedly follow ~20 and ~60 year quasi-periodicities. The contribution of large sunspots to the whole activity can also be related to the properties of quasi-biennial oscillations [8,9]. Mandal and Banerjee [3] worked with the solar cycle strength defined through the total area of specific sunspots emerging during the cycle. According to [3], analyzing cycles 16 to 23, sunspots with areas between 200 and 500 MH contribute more to odd cycle numbers. Nevertheless, Mandal and Banerjee [3] argued that only large sunspots represent the main indicators of solar activity and help quantify the asymmetry between solar hemispheres. On the decadal-to-centennial scale, the secular Gleissberg cycle (see [10–12] among others), modulating the amplitude of the solar cycle, affects the long-term properties of sunspots in a different way depending on their size and governs the sunspot formation in general [2,3].

Large and small sunspots are thought to represent the large- and small-scale components of the solar dynamo [3,13]. Obridko and Badalyan [2] conjectured that the formation of large sunspots occurs in the subsurface layers of the Sun, whereas small sunspots are connected to the deep dynamo. The state of the art in dynamo modeling allows model sequences of the sunspots to be generated. These artificial sunspots follow not only the basic regularities but also some of the long-term irregularities of solar activity [14]. The suggested algorithms producing artificial sunspots differ in where the flux originated and how it is transferred through the convection zone [15–17]. As the algorithms are driven by the observations of real sunspots, a better understanding of their relevant features, to be reproduced by the models, is required.

The identification of recurrent sunspot groups performed by Nagovitsyn et al. [7] to uncover the relationship between their area and lifetime complements earlier efforts to produce the catalogue of long-lived groups [18,19] and follows the opinion of Ringnes [20] who argued that “a revised catalogue of recurrent spots ... would ... be very desirable”.

This paper tackles the contribution of large sunspots to general solar activity on annual-to-multi-decadal scales in quantitative and qualitative ways. Addressing this challenge, we construct an algorithm aimed to identify large and moderate recurrent sunspot groups from the Royal Greenwich Observatory (RGO, 1874–1975) and Solar Optical Observing Network (SOON, 1976–2020) daily databases. Designing the details of the identification algorithm, we are motivated to trace the manifestation of strong magnetic field in the same location for several solar rotations. The identified groups, i.e., the groups selected by the algorithm, form so called nestlets (first, introduced by Henwood et al. [19] for a similar purpose). The identification leads us to proxies of strong magnetic field, which are the composites of the solar activity defined as the 11- or 22-year smoothing of the daily area of the sunspot groups included into the constructed nestlets. The temporal variations of the composites compared with general solar activity and the lifetime of the sunspot nestlets constitute the content of the paper, which is structured in a standard way. Sections 2 and 3 describe the data and the method. Results are presented in Section 4. The discussion is in Section 5. Section 6 concludes. Technical details of the identification algorithm and its detailed comparison with the expert identification of the recurrent groups by [18] and earlier algorithms by Henwood et al. [19] and Nagovitsyn et al. [7] are relegated to the Appendices A–D.

## 2. Data

We use the daily series compiled by the Royal Greenwich Observatory (RGO) from 1874 to 1976 and the US Air Force from its Solar Optical Observing Network (SOON) from 1976 onward [10]. The joint catalogue contains 41394 different groups according to their IDs.

The change in the place and facilities of the observation brings inconsistency into the joint RGO/SOON database ([21,22]). The methods of the data processing including the SOON practice of rounding down the limb-area correction factors also affect the consistency of the joint catalog. The web sites <https://solarscience.msfc.nasa.gov/greenwch.shtml> (accessed on 5 January 2022) and <http://solarcyclescience.com/activeregions.html> (accessed on 5 January 2022) ([23]) contain RGO/SOON sunspot group data from 1874 onward. Hathaway et al. [24] defined the correction factor 1.4 for the SOON areas (i.e., the areas associated with 1976 and later years). We denote  $\mathbf{D}$  the set of the sunspot groups from the joint RGO/SOON catalogue.

The choice of the databases is worth commenting on. Great many efforts have been recently made to improve the indices of solar activity (see, e.g., [25–27]). The homogeneity of the RGO time series in 1880–1920 were recently questioned and, as a result, the corrections were proposed by Willis et al. [28], Cliver [29]. Clette et al. [30] produced the second version of ISSN adjusting so called observer factor in the definition of the Wolf numbers and working through the discontinuity in the time series, thought to be performed with the Wolf numbers in 1945. Several composites have been built on the sunspot groups: the group

sunspot number by Hoyt and Schatten [31] and its extension by Lockwood et al. [32], the “backbone” group number reconstruction by Svalgaard and Schatten [33], and the group number derived by Usoskin et al. [34]. Our choice of the RGO/SOON database is motivated by the requirement to deal with a long time series which contain the position of the spots together with the characteristic of the activity strength.

### 3. Method

#### 3.1. Focus of the Identification

Large recurrent sunspot groups give a relevant proxy to the strong magnetic field of the Sun manifested at specific locations for weeks. However, the identification of the recurrent groups is uncertain since they are not observed at the “back” side of the Sun (at least, until Solar Terrestrial Relations Observatory, STEREO, [35] and Solar Dynamics Observatory [36] started recording the solar surface invisible from the Earth). Henwood et al. [19] referred to the results of their identification of recurrent groups as nestlets. In contrast to Henwood et al. [19], we focus on the identification of large and moderate recurrent groups and end up with large and moderate nestlets. As we will show later in detail, the design of our identification can lead to errors when a genuine “old” group is vanishing at the appearance on the solar disk but another larger group emerging nearby is included to the nestlets or no groups are identified at all. In the first case, the identification modifies the notion of nestlets introduced by Henwood et al. [19] through an increase of their size. In the second case, the vanishing part of sunspot groups (or the whole group if it returns to the solar disk for the first time) is not included into our nestlets. The identification of disappearing recurrent groups seems to rise uncertainties whereas their contribution to the solar activity associated with the nestlets is minor. As a result, we are biased to omit a minor contribution but avoiding potential erroneous identifications.

#### 3.2. Identification of the Recurrent Groups

The rotation period of the Sun is approximately 27 days. The exact value depends on the latitude, as the Sun exhibits the differential rotation. If a sunspot group leaving the solar disk appears on it once more this occurs  $\sim 14$  days later in a neighborhood of the point with the same Carrington coordinates (i.e., the coordinates related to the Sun). The explicit position is affected primarily by a slow drift of the sunspots across the Sun estimated in up to 0.01–0.03 degrees per day [37,38]. Rare chaotic jumps in the records of specific sunspot groups are mainly explained by errors [39]. However, the appearance or disappearance of sunspots within a group also affects the reported group position. As a result, a new occurrence of recurrent groups are expected in an ellipse centered at the longitude and latitude of the previous observation. Referring to the ellipse, we mean the points on the two-dimensional plane consisting of the latitudes and the longitudes, which are not related to the embedding of the Sun in the real three-dimensional space. We specify the ellipse in the following way.

Let  $P = 27.2757$  be the Carrington rotation period that represents a certain average of the periods observed because of the differential rotation of the Sun. Then we put  $\Delta = 13.2 \approx 360/P$ . This  $\Delta$  roughly represents the move of each group per day across the solar disk caused by the (differential) solar rotation.

Further, we consider the sunspot groups with the longitude located in the range  $S_r = [90^\circ - 2\Delta, 90^\circ - \Delta]$  and focus on those that the maximum of their recorded areas exceeds some relatively large threshold  $A$ . These groups are going to leave the disk two days later (if they still exist). Let  $G_1$  be one of these groups observed at some time  $t_1$  (measured in days) with the longitude  $x_1$  from the range  $S_r$ , the latitude  $y_1$ , and the area  $a_1$ . For the sake of simplicity in the notation, the identification procedure is explain just for  $G_1$ . We intend to look for its new appearance at the left of the solar disk 16.5–17.5 days later. Let  $G_2$  be a group observed at  $t_2 \in [t_1 + 16.5, t_1 + 17.5]$  days. Then we introduce the ellipse centered at the Carrington coordinates  $(x_1, y_1)$  of the group  $G_1$  and endowed with some semi-axes  $l_x$  and  $l_y$ , which are the parameters of the procedure that has to be adjusted and

fixed. If  $G_2$  is located within the ellipse, it is a candidate to be identified with the group  $G_1$ . Each group  $G_1$  can have either 0, or 1, or more such candidates. The group  $G_1$  is claimed to be non-recurrent in the first case. A single candidate is identified as  $G_1$  in the second case. The group with the area being closest to the area  $a_1$  of  $G_1$  is identified with  $G_1$  in the third case.

Eventually, we choose the semi-axes to minimize the errors of the identification. To this end, we use the sunspot groups that drift 7–10 days along the solar disk. With the threshold  $A = 950$  MH and the groups observable at least 10 consecutive days, the semi-axes  $l_x$  and  $l_y$  are adjusted via the maximization of the  $F_1$ -score:  $F_1 = \frac{tp}{tp+0.5(fp+fn)}$ , where  $tp$ ,  $fp$ , and  $fn$  are the numbers of the true positive, false positive, and false negative outcomes of the identification. The adjusted values  $12^\circ$  and  $5^\circ$  of the longitudinal and latitudinal widths of the semi-axes are stable with respect to the drop of  $T$  from 10 to 7 days. This stability in  $T$  favors the application of the adjusted values to the real identification when  $T \approx 17$ . The details of the algorithm are described in the Appendices A–D.

### 3.3. Samples of Large and Moderate Nestles

We extract two sub-catalogues of the groups included into the nestlets with our identification algorithm. Let  $\mathbf{L}$  be extracted sunspot groups from  $\mathbf{D}$  such that the maximum of their recorded areas is more than 950 MH. Let  $\mathbf{M}$  be extracted sunspot groups from  $\mathbf{D}$  such that the maximum of their recorded areas is between 700 and 950 MH. Then the sub-catalogues  $\mathbf{L}$  and  $\mathbf{M}$  are our large and moderate nestlets. Controlling the necessity to deal with just large recurrent sunspot groups, we also consider two other sets  $\mathbf{H}$  and  $\mathbf{LH}$  of large sunspot groups. The set  $\mathbf{H}$  consists of all (non-necessary recurrent) sunspot groups from  $\mathbf{D}$  such that the maximum of their recorded areas is more than 950 MH. Note that big non-recurrent groups from  $\mathbf{H}$  do not belong to  $\mathbf{L}$ . Regarding the opposite exclusion, if a recurrent group  $G \in \mathbf{L}$  is obtained as the identification of two groups  $G_1$  and  $G_2$  and, for example,  $G_2$  does not show up an area greater than 950 MH, then only  $G_1$  is in  $\mathbf{H}$ , but  $G_2$  is not. The set  $\mathbf{LH}$  is the union of  $\mathbf{H}$  and  $\mathbf{L}$ . It is defined to exhibit the transition between conclusions obtained with  $\mathbf{L}$  and  $\mathbf{H}$ .

We explore the time series which consist of consequent daily areas of sunspot groups averaged over 11-year sliding windows. The daily areas are taken from the samples  $\mathbf{D}$ ,  $\mathbf{L}$ ,  $\mathbf{M}$ ,  $\mathbf{H}$ , and  $\mathbf{LH}$ . Their averages are measured in MH per day. Formally, let  $\Omega \subseteq \mathbf{D}$  be the set of sunspot groups and  $a_\Omega(d)$  be the total area of all sunspot groups from  $\Omega$  associated with day  $d$ . Then we put

$$R_\Omega(t) = \frac{1}{N} \sum_{d \in [t-(N-1)/2, t+(N-1)/2]} a_\Omega(d), \quad \Omega \in \{\mathbf{M}, \mathbf{L}, \mathbf{H}, \mathbf{LH}\}, \quad (1)$$

where  $N = 4017$  is the length of the 11-year moving window, and denote  $R_{\text{ISSN}}(t)$  the 11-year moving average of index ISSN (International Sunspot Numbers obtained from WDC-SILSO, Royal Observatory of Belgium, Brussels, [40], <http://www.sidc.be/SILSO/> (accessed on 5 January 2022)). With these composites, we discuss the contribution of the relatively large sunspot groups to the solar activity. The composite  $R_{\mathbf{LH}}$  is used to describe the change in the dynamics of the composites as  $R_{\mathbf{L}}$  substitutes  $R_{\mathbf{H}}$ .

The time series  $R_{\mathbf{M}}$  and  $R_{\mathbf{L}}$  constitute a part of the series  $R_{\mathbf{D}}$ . According to Figure 1, these parts are well correlated with the full series. As is well known, the smoothed ISSN are also correlated with  $R_{\mathbf{D}}$  (red and blue curves). In particular, all four curves attain a global minimum, a global maximum, and a second maximum at cycles 13–14, 18–19, and 21–22, respectively (Figure 2). We note that the variability of  $R_{\mathbf{M}}$  (orange curve) is smaller than that of  $R_{\mathbf{L}}$  (magenta curve).

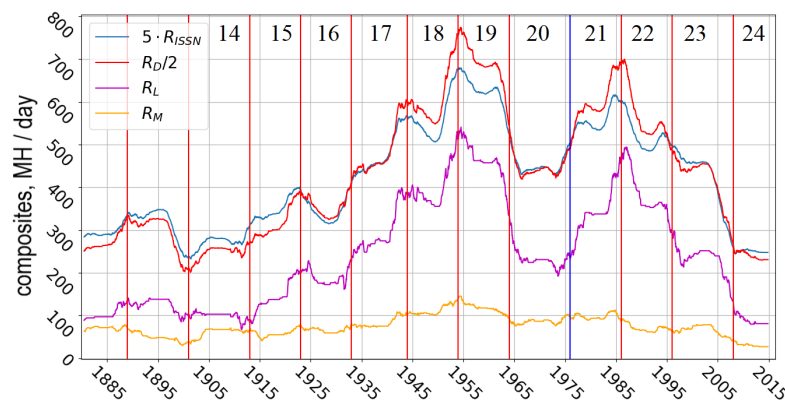


**Figure 1.** The 11-year moving averages  $R_{ISSN}$ ,  $R_D$ ,  $R_M$ , and  $R_L$  of index ISSN and the areas of all, medium, and large selected sunspots, respectively, in line with (1);  $R_{ISSN}$  and  $R_D$  are scaled to fit the Y-range.

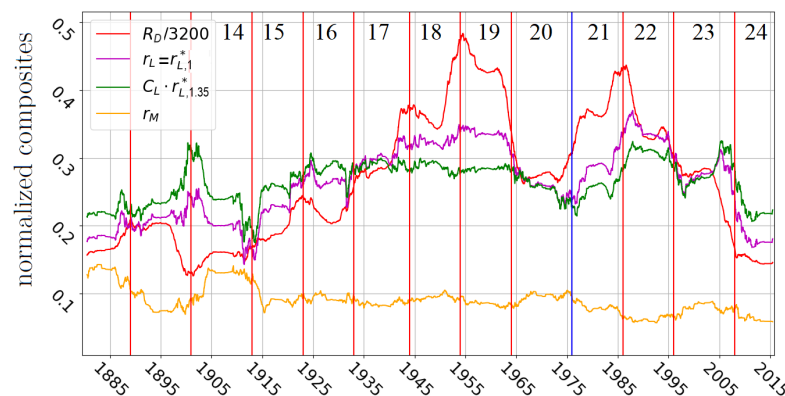


**Figure 2.** The normalized composites  $r_M = R_M/R_D$  and  $r_L = R_L/R_D$  of the areas of the moderate and large selected sunspot groups; specific normalization  $r_{L,1.35}^* \sim R_L/R_D^{1.35}$  and the composite  $R_D$  of the areas of the all sunspots (both rescaled by an appropriate constant  $C_L$  and number  $1/3200$ , respectively).

Estimating the contribution of the different components of  $R_D$  to the full index, we normalize the series  $R_M$  and  $R_L$  into two new series:

$$r_\Omega = \frac{R_\Omega}{R_D}, \quad \Omega = \mathbf{L}, \mathbf{M}, \quad r_{\Omega,\beta}^* = \frac{R_\Omega}{R_D^\beta} \quad \Omega = \mathbf{H}, \mathbf{LH}, \mathbf{L}, \quad (2)$$

where the exponent  $\beta$  is adjusted for each composite separately to obtain the flattest graph of  $r_{\Omega,\beta}^*$  with the data of cycles 16–19 (the deviation from the mean value for these data is minimized with the step of 0.01 in the values of  $\beta$ ). The adjusted values of  $\beta$  are 1.20, 1.19, and 1.35 for the composites **H**, **LH**, and **L**, respectively.

#### 4. Results

##### 4.1. Indices of Recurrent Sunspot Groups

The normalized large selected sunspot groups  $r_L$  (the magenta curve in Figure 2) still followed  $R_D$  after 1915, thus, contributing disproportionately strongly to the overall solar activity. This disproportionality can be assessed quantitatively by using the time series  $r_{L,\beta}^*(t)$  defined through the normalization by the power function, Equation (2). This  $r_{L,\beta}^*(t)$  (green curve in Figure 2 obtained with  $\beta = 1.35$  and shifted via the multiplication by an appropriate factor to uplift it to the range of the values of the other curves) exhibits quasi-constant behavior when  $t$  is located in 1925–1965, cycles 16–19. The adjusted value of  $\beta$  is not important itself. We emphasize here the very possibility to quantify the specific

contribution of the large selected sunspot groups during 4 cycles in a row in a simple way. The variability of  $r_{L,\beta}^*$  was larger before 1925 and after 1965. Nevertheless, the values of  $r_{L,\beta}^*$  equaled to  $\sim 0.25$  (in the units of Figure 2) were attained in cycles 14, 15, 20, and 21, which is not far from the values 0.28–0.30 observed during cycles 16–19.

The weak variability of the normalized composite  $r_{L,\beta}^*$  is observed with the range of  $\beta$  from [0.3, 0.4], where 1.35 is the best estimate. This property characterizes just the large selected sunspot groups. The variability of the normalized composite  $r_{H,\beta}^*$  built on the large (but not necessarily recurrent) groups is stronger (the black curve on Figure 3). The composite  $LH = L \cup H$  collects features of both datasets. As a result, the deviation from the mean value of  $r_{LH,\beta}^*$  is between that of  $r_{L,\beta}^*$  and  $r_{H,\beta}^*$ . The standard deviation computed with  $L$  is less than that found with  $LH$  and  $H$  on the cycles 16–19. The shift of the optimal exponent of 1.35 toward 1 for the normalized composites  $r_{H,\beta}^*$  and  $r_{LH,\beta}^*$  emphasizes the role of just recurrent groups (selected to the nestlets) in their disproportionate contribution to solar activity.

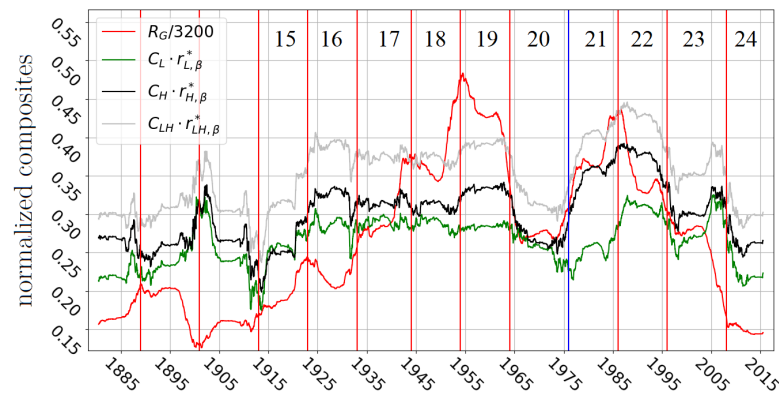


**Figure 3.** The composites  $r_{H,\beta}^*$  (black),  $r_{LH,\beta}^*$  (gray),  $r_{L,\beta}^*$  (magenta) obtained through the normalization (2) with a power function  $r_D^\beta$  of the activity, where  $\beta$  equalled to 1.20, 1.19, and 1.35, respectively, is adjusted to each composite separately. Scaled solar activity given with the index  $R_G$  (red) and the boundaries of the solar cycles (vertical lines) are for illustrative purposes.

The normalized moderate selected sunspot groups  $r_M$  demonstrated quasi-constant behavior in 1915–1975 followed by slow variations from 1975 onward (the orange curve in Figure 2). In general, the  $r_M$  and  $r_{L,1.35}^*$  curves exhibited an anti-correlation (most clearly observed with the 1965–1997 data). Interestingly, the change from  $r_{L,1.35}^*$  to  $r_L$  weakens the anti-correlation despite the fact that the composites  $r_M$  and  $r_L$  correspond to each other by definition. During the short interval from 1898 till 1903 and later from 1997 till 2010,  $r_M$  and  $r_{L,1.35}^*$  varied co-directionally. New data allow us to estimate a further agreement between  $r_{L,1.35}^*$  and  $r_M$ .

#### 4.2. Recurrent Sunspot Group Lifetime

Blanter et al. [41] claimed that the lifetime of sunspots increased by factor 1.4 during 1915–1940. They obtained this result indirectly when simulating the solar activity with a modulated AR-1 process. Henwood et al. [19] confirmed this prediction identifying the recurrent sunspot groups from the catalogue known as Greenwich Photo-heliographic Result (GRP), <https://www.ngdc.noaa.gov/stp/solar/greenwich.html> (accessed on 5 January 2022). We are able to reproduce the dynamics of the lifetime exposed by Henwood et al. [19] with our recurrent sunspot groups. This supports the reliability of our methodology and allows us to make an additional conjecture regarding the lifetime of large recurrent sunspot groups.

We note that the identification of large recurrent groups leads to the modification of the initial catalogue  $D$ : the components of the large selected groups are combined, whereas the rest of the groups are left as they are. Let  $D'$  be the modified catalogue. Further, following

Henwood et al. [19], if several groups from  $D'$  share the day of the first record, only the group with the largest lifetime is kept and the other groups are eliminated. We denote  $D'' \subset D' \subset D$  the resulting catalogue. The lifetime of each group from  $D''$  with the first and the last records separated from the limb on at least  $2\Delta^\circ$  is the time difference between them increased by 1 day. If the first or the last records are offset from the limb on less than  $2\Delta^\circ$  then 8 days are added to the time difference between these records (or 7 days if the offset is less than  $\Delta^\circ$ ). For any 22-year window the lifetime  $\mathcal{T}_g$  of each group  $g$  associated with this window is summed up and divided by  $22 \cdot 365.25$ . The result introducing the lifetime per day is denoted  $\tau_{D''}$  and assigned to the center of the window:

$$\tau_{D''}(d) = \frac{1}{22 \cdot 365} \sum_{d_{0g} \in [d-11 \cdot 365, d+11 \cdot 365-1]} \mathcal{T}_g,$$

where  $d_{0g}$  represents the day of the group  $g$ 's first record. In words,  $\tau_{D''}$  represents the average number of the days such that the groups from  $D''$  exist in the Sun. The 22-year windows are used to follow Blanter et al. [41] and Henwood et al. [19]. The same definition of the lifetime applied to the catalogues  $M$  and  $L$  returns us the normalized lifetime per day naturally called  $\tau_M$  and  $\tau_L$  (i.e., the average number of the days such that the groups from  $M$  and  $L$ , respectively, exist in the Sun).

The normalized lifetime per day  $\tau_{D''}$  shown in Figure 4 in blue and obtained with the approach of paper [19] but with our identification of the recurrent groups repeats the graph constructed by Henwood et al. [19]. The right endpoint of the graph from paper [19] corresponds to 1965, 11 year prior to the move of the observation place occurred in 1976. As a result of this move, the number and the area of the sunspots increased. Corrections were introduced to calibrate the indices of solar activity based on the sunspot groups [21]. However, these corrections do not calibrate the lifetime. Therefore, the comparison of the parts located before 1965 and after 1987 are impeded. We can note based on the right part of the graph itself, that a decrease in  $\tau_{D'}$  started when the sliding window reached the descending phase of cycle 23. This decrease turned to the fall when the data of cycle 24 were substituting for the data of cycle 22 in the sliding window.

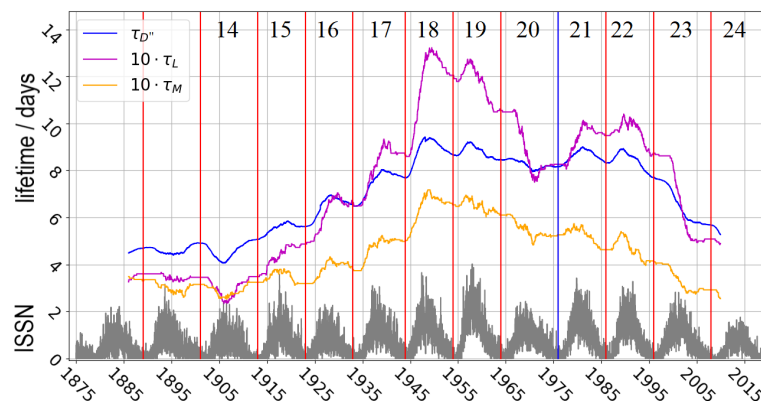


**Figure 4.** The 22-year moving averages  $\tau_{D''}$  (in blue),  $\tau_L$  (in magenta), and  $\tau_M$  (in yellow) of the lifetime per day calculated for the groups from the catalogues  $D''$ ,  $L$ , and  $M$  representing large recurrent sunspot groups, moderate recurrent sunspot groups and all groups recorded after the identification and related to that examined in [19]. Daily ISSN (scaled) is in black.

The lifetime composites  $\tau_L$  and  $\tau_M$  derived from only large and, respectively, only moderate recurrent sunspot groups follow the rises and falls of  $\tau_{D''}$ . The graphs of  $\tau_L$  and  $\tau_M$  look like a scaled version of  $\tau_{D''}$ . The  $\tau_M$  graph contains a secular wave with the maximum at cycles 18–19, which resembles the Gleissberg cycle. The anomalous 20th cycle affects mostly the composite  $\tau_L$  that characterizes the large selected sunspot groups, causing a drop followed by a rise which violates a steady decrease of the wave of the

Gleissberg cycle. The adequate calibration of the lifetime has to shift the right (i.e., after 1976) part of the composites downward, but the exact position has not been determined yet. Nevertheless, the peculiarities of our identification algorithm, which matches the components with similar areas, makes the inconsistency related to large recurrent groups smaller. Therefore, the calibrated right part of the (blue)  $\tau_{D''}$  graph might fall at the right end to the level of the beginning of the 20th century, thus staying in line with the existence of the Gleissberg-cycle wave (which seems to be the case for  $\tau_M$ ). On the contrary, the fall of the (magenta)  $\tau_L$  at the right to the level attained a century ago seems very unlikely.

## 5. Discussion

This paper reveals new regularities and irregularities of solar activity on the decadal-to-multi-decadal scale. Applying a machine learning technique to identify large recurrent groups from the daily 1874–2020 RGO/SOON catalogue we select the nestlets of sunspot groups and examine a proxy  $R_L$  of solar activity defined as the daily area of these groups averaged over 11 years. This proxy  $R_L$  is a part of the index  $R_D$  which represents the 11-year moving average of the daily areas of all sunspot groups. The index  $R_D$  is related to various strongly correlated proxies of solar activity, discussed in details, for example, by Lockwood et al. [26], which are inferred from the sunspot groups. The construction of the nestlet catalogue complements efforts performed to produce and calibrate records of solar activity [26,27,33,34,42,43].

We posit that the indices  $R_L$  and  $R_D$  exhibit a strong correlation (Figure 1). The contribution of large sunspot nestlets to solar activity is established to be disproportionately strong in terms of the relationship between  $R_L$  and  $R_D$  (Figure 2). The disproportionality is estimated quantitatively by the normalization of the index  $R_L$  by the power function  $R_D^\beta$  of the full index. The proportional contribution is given by the exponent  $\beta = 1$ . However the normalization with  $\beta = 1$  does not exclude a positive correlation with solar activity. A larger exponent is required, which is  $\beta \approx 1.35$ . The normalized time series  $r_L^*$  exhibited a fixed level during cycles 15–19 and attained the values close to this level in cycles 14 and 20–23 (Figure 2). We stress that the preliminary selection of the recurrent groups is important to quantify the properties of the large sunspot groups. The composite  $R_H$  built on the large sunspot groups from the initial catalogue still contributes to the overall activity disproportionately strongly, but weaker than  $R_L$  does. The normalization of  $R_H$  to  $r_{H,\beta}^*$  by a power function of the full index  $R_D$  that intends to flatten the graph within cycles 16–19 requires the exponent  $\beta = 1.19$  being closer to 1 than 1.35 and results in a less flatter part of  $r_{H,1.19}^*$  than that of  $r_{L,1.35}^*$  (Figure 3). The peculiar role of the largest sunspots found here is in line with the conclusions of other papers [3,44–46].

Our additional empirical findings are based on the fraction  $\tau$  of days such that the sunspot nestlets exist in the Sun. These fractions are computed within 22-year sliding windows. The strongest contribution of the large sunspot nestlets to the overall solar activity occurred during its second largest maximum in cycles 21–22 (see  $R_L$  and  $r_L^*$  curves in Figures 1 and 2, respectively) when the fraction  $\tau_L$  of the days with these large nestlets exhibited rather regular values (Figure 4). Thus, the maximum of  $R_L$  occurred in cycles 21–22 was driven primarily by the growth in the area of the largest groups rather than in their number per day.

The moderate nestlets are characterized by the indices  $R_M$  and  $\tau_M$ , which represent the 11-year average of their daily areas and 22-year average of their number per day, respectively. The ratio of  $R_M$  to the full index  $R_D$  exhibited a constant level in cycles 15–19 and a strong anti-correlation with the normalized index  $r_{L,1.35}^*$  (Figure 2). The deep minima of solar activity observed in  $\sim 1900$  and 2008 are characterized by the short termination of the anti-correlation between large and moderate long-lived sunspot group composites and co-directional changes in the two series. These episodes may signal the beginning of a new Gleissberg cycle. We note that moderate non-recurrent sunspot groups attained the main maximum in cycles 21–22 [2], in contrast to the recurrent groups. We support the conjecture by Henwood et al. [19] regarding the existence of the Gleissberg cycle in the

dynamics of the lifetime (with the quantity that they introduced), arguing that the index  $\tau_M$ , which represents the average daily number of the moderate nestlets observed in the Sun, followed a secular wave with minima in approximately 1906 and 2005. Moreover, the index  $\tau_M$  is characterized by rather extent previous minimum of the Gleissberg cycle around 1900 (Figure 4). Therefore, the presented results suggest that the minimum of the centennial cycle started in solar cycle 23 and followed by solar cycle 24 may be long without actually entering a Grand Minima epoch. In this case, we should not expect a quick return of solar activity to the high level recorded in the mid of 20th century. The study of the average lifetime of different recurrent sunspot groups, which is more natural characteristic than the fraction  $\tau$ , can shed more light on the properties of the Gleissberg cycle. But this is worth doing in a separate study.

Our identification of the recurrent groups is similar to that performed by Nagovitsyn et al. [7], but we focus on moderate and large groups ending up with a more accurate identification of just these groups with at least the training set related to the visible part of the Sun, Figure A1. With 1944–1976 year data, a turn from  $12^\circ \times 2^\circ$  (related to [7]) to  $12^\circ \times 5^\circ$  ellipse reduces the number of errors from 15 to 3 (see Table A2 with the complete list of the IDs of the groups related to the errors). As the drift of sunspot groups depends on their area [10], one may adjust the dependence of the ellipse axes on the area of the recurrent sunspots when identifying all recurrent sunspot groups. The direct comparison between the results obtained with our and Henwood et al. [19]’s identification procedures is not well defined, as nobody knows what groups are indeed recurrent. As an example, we take 8 groups which are observed in 1986, called recurrent by Henwood et al. [19], and satisfied our criteria of the moderate/large group identification. All of them are indeed identified as recurrent by our algorithm (see Appendix C). Furthermore, the conclusions regarding the solar proxies built on the identified groups are comparable, and we completely reproduce the dynamics of the lifetime found by Henwood et al. [19] with the 1874–1976 data (Figure 4). The reproduction of the time variability of the lifetime found by Henwood et al. [19] and Blanter et al. [41] gives additional credibility to our identification mechanism.

Our large and moderate nestlets are related to but differ from sunspot nests, active regions, active longitudes, and complexes of activity. The nests were defined by Castenmiller et al. [47] as the groups of sunspots that keep their location during 6–15 solar rotations. The sunspot nests and the other terms reported above are introduced to describe the persistence of the strong magnetic field at fixed location (region, longitude) in the Sun (see [48–50] among others). This phenomenon can be associated with several sunspot groups of different sizes located within a broad region, in contrast to a single group found in smaller regions and selected to the nestlets.

## 6. Conclusions

We have emphasized that large recurrent sunspot groups contributed disproportionately strongly to the overall solar activity in 1915–2005, probably except a neighborhood of 1975. The 11-year moving average  $R_L$  of the areas of these groups normalized to  $r_{L,\beta}^* = R_L/R_D^\beta$  by the 11-year moving average  $R_D$  of the areas of all groups with the exponent  $\beta = 1.35$  exhibited a weak variability around a constant level during cycles 15–19, thus, giving evidence for the estimate  $R_L \sim R_D^{1.35}$ . The quasi-constant behavior of  $r_{L,\beta}^*$  was followed by a drop in the anomalous cycle 20 and a rise to its global maximum in cycles 21–22. The average fraction  $\tau_L$  of the days with the large nestlets in the Sun kept exhibiting regular values at the time of this maximum of  $r_{L,\beta}^*$ .

In contrast to the large selected sunspot groups, the moderate ones followed the solar activity as it was:  $R_M \sim R_D$ , whereas the pattern of their active days given by  $\tau_M$  resembled the Gleissberg cycle with minima at the beginning of the 20th and 21st centuries.

The particular role of the long-lived sunspot groups highlighted in this paper may be explained by interactions of two multi-scale processes which contribute to solar dynamo. One process is explicitly connected to the global component of the dynamo being responsi-

ble for the sunspot formation. The other is related to the turbulent diffusion destroying the sunspots. One may assume that the sunspot formation process continues with the development of the sunspots in the Sun. The sunspot area enlarges when the spots rise into the surface layers from the base of the convective zone. The growth in the area remains regular while the moderate recurrent sunspot groups are created. The regularities of this creation found in this paper are probably governed by the Gleissberg cycle. However, the largest sunspot groups, which are extreme events in the probability distribution of the sunspot groups with respect to their areas [46], exhibit more complex behavior, as derived here and by other authors (see [2,3,13]). Better understanding of the processes related to the amplification of the magnetic field in the surface layers may shed light on the anomalous contribution of the largest recurrent sunspot groups to the overall activity.

**Funding:** This research received no external funding.

**Institutional Review Board Statement:** Not applicable.

**Informed Consent Statement:** Not applicable.

**Data Availability Statement:** The data used in this paper are freely available at <https://solarscience.msfc.nasa.gov/greenwch.shtml> (accessed on 5 January 2022) and <http://solarcyclescience.com/activerregions.html> (accessed on 5 January 2022).

**Acknowledgments:** I express my deepest gratitude to Vladimir Fufaev who designed the computer code extracting nestlets from the database. I am also thankful to Mikhail Shnirman for fruitful discussions during the work on the paper.

**Conflicts of Interest:** The author declares no conflict of interest. The funders had no role in the design of the study; in the collection, analyses, or interpretation of data; in the writing of the manuscript, or in the decision to publish the results.

### Appendix A. Rules Applied to Define Recurrent Sunspot Groups

In this section, we describe in detail the algorithm which is designed to identify large and moderate recurrent sunspot groups. These groups are extracted from the catalogue **D** of RGO/SOON records that contain the Carrington coordinates of the groups, the observed area, and the observation time, among other characteristics.

Let us number the groups from **D**:  $G_1, G_2, \dots$ . A sunspot group  $G_k$  numbered by  $k$  is described by the sequence of all its records  $\{g_{k,1}, \dots, g_{k,N_k}\}$ , where  $N_k$  is the number of records and  $g_{k,j}$  consists of the longitude  $x_{k,j}$ , latitude  $y_{k,j}$ , area  $a_{k,j}$  and time  $t_{k,j}$  of the observation (accurate to a thousandth of a day). The coordinates  $x$  and  $y$  considered in the Stonyhurst system in the above notation are transformed from the Carrington coordinates given in the records [51]. Note, the Carrington-to-Stonyhurst transformation is inverse to one that is applied to design the records of the sunspot groups. The origin in the Stonyhurst system is located at the intersection of the Sun’s equator and the central meridian as seen from the Earth. Therefore, the pairs of observed sunspot groups’ longitude and latitude are expected to belong to the square  $[-90^\circ, 90^\circ] \times [-90^\circ, 90^\circ]$ . We recall that each sunspot group moves approximately  $\Delta = 13.2^\circ$  per day across the solar disk because of solar rotation.

Two groups from **D** are identified as matching parts of a single recurrent group in the following case. The first group  $G_k$ , called further a source, has a record  $g_{k,j}$  with the longitude  $x_{k,j}$  located in the section  $[90^\circ - 2\Delta, 90^\circ - \Delta]$ . The second group  $G_m, m \neq k$ , is expected to be observed after  $T = 17$  days inside the corresponding region. The following rule reformulates this in a more rigorous way.

**Rule 1.** Let  $l_x$  and  $l_y$  be two positive parameters that will be specified later. The group  $G_m$  is called the complement of the source group  $G_k$ , if it has a record  $g_{m,p}$  such that the recorded time  $t_{m,p}$  belongs to the day-long interval centered at  $t_{k,j} + T$ , i.e.,

$$-0.5 \leq t_{m,p} - (t_{k,j} + T) \leq 0.5, \tag{A1}$$

and the coordinates  $x_{m,p}, y_{m,p}$  are located inside the ellipse in the  $xy$ -plane with semi-axes  $l_x$  and  $l_y$ . This ellipse is centered at the point with the latitude  $y_{k,j}$  and the longitude  $x_{k,j}$  shifted by  $\Delta x = (T + (t_{k,j} - t_{m,p})) \cdot \Delta \text{ modulus } 360 = (T + (t_{k,j} - t_{m,p})) \cdot \Delta - 360$ :

$$\frac{(x_{k,j} + \Delta x - x_{m,p})^2}{l_x^2} + \frac{(y_{k,j} - y_{m,p})^2}{l_y^2} \leq 1. \tag{A2}$$

The center of the ellipse has approximately the same Carrington coordinates as those from the record  $g_{k,j}$ .

**Rule 1'.** If the large recurrent groups are searched for, the recorded area of the complement  $G_m$  has to be larger than a threshold  $A$  fixed to 100 MH:  $a_{m,k} > A$ .

Rules 1 and 1' do not provide the uniqueness of the complement. Resolving the multiplicity problem, we impose the following rule.

**Rule 2.** All possible sources are arranged in descending order with respect to the areas of the groups. If Rule 1 allows us to put several complements into correspondence with a source, then the group with the largest area is chosen as the complement.

Once the source  $G_j$  and the complement  $G_m$  are matched by the algorithm, the records of  $G_m$  are assigned to  $G_j$  (and  $G_m$  is excluded from further consideration).

We need to say a word about the search for the complement of those groups that have already been identified as recurrent with Rules 1 and 2 (i.e., the third and consequent returns of the groups to the solar disk are the goal of the identification). Formally, when the group is identified as recurrent, the search for the next complement is fully defined by Rules 1 and 2. However, we introduce an additional

**Rule 3.** The complement is searched only for such (already identified) recurrent groups that the maximum of their areas does not exhibit a large drop from the penultimate to ultimate appearances. Namely, let  $a_{-1}$  and  $a_0$  be the maxima of the areas during the penultimate and ultimate appearances of a solar group  $G_k$ . Then the complement is searched for  $G_k$  if  $a_0 > 0.5a_{-1}$ .

The purpose of Rule 3 is to trace each recurrent group to its complete disappearance. As is well known, when sunspots start decaying they do it rather quickly (Petrovay and van Driel-Gesztelyi [52] quantified the sunspot decay). Then a recurrent group shrunk to less than a half of its maximal area is likely to disappear before its next appearance. There are no exact rules that distinguish between small recurrent and "new born" groups at the limb. In rare cases, we erroneously neglect the last fragment of a recurrent sunspot group.

The contribution of the last fragment to the composites  $R_L$  and  $R_M$  is small and, therefore, the complication of the identification at this stage seems unnecessary.

In rare cases, the group can attain the threshold  $A_L$  or  $A_M$  of moderate or large sunspot groups at the non-first appearance on the solar disk. We account for this possibility by performing a search for a backward complement in the following way.

**Rule 4.** Let the group  $G_k$  from the initial catalogue  $\mathbf{D}$  with  $\max_k a_{k,j} > A_\Omega$ , where  $\Omega$  is  $\mathbf{L}$  or  $\mathbf{M}$ , be observed near the limb, i.e.,

$x_{k,j} < -90^\circ + \Delta$ . Then the source  $G_s$  of  $G_k$  is searched in the ellipse defined by (A2) (but the notation is different, as  $G_k$  plays the role of the complement) with the additional requirement  $\max_p a_{s,p} > 0.75 \cdot \max_j a_{k,j}$ .

Rules 3 and 4 represent the observation that typical sunspot groups quickly attain the maximum but decay slowly. We verify that the constants 0.5 and 0.75 from conditions 3 and 4, which look somewhat arbitrary, are flexible.

### Appendix B. Choice of the Ellipse Semi-Axes

Further, we explain the choice of the parameters. In order to adjust the semi-axes  $l_x$  and  $l_y$  of the ellipse, we introduce the training set

$$\Omega_{A,T} = \{G_k \in \Omega : \max_{j=1,\dots,N_k} a_{k,j} > A, x_{k,1} > -90 + \Delta, x_{k,1} + T\Delta < 90 - \Delta\}, \quad (A3)$$

which consists of sunspot groups  $G_k, k = 1, 2, \dots$ , such that their maximal observed area is larger than  $A$  and the location of the first recorded position rotates with the Sun to a point which is still visible from the Earth. We distinguish between the recurrent and non-recurrent groups in the training set:

$$\Omega_{A,T}^+ = \{G_k \in \Omega_{A,T} : t_{k,N_k} - t_{k,1} \geq T - 0.5\}, \quad \Omega_{A,T}^- = \Omega_{A,T} \setminus \Omega_{A,T}^+.$$

The supervised training is well defined for the training set, where  $\Omega_{A,T}^+$  determines the target of the identification. The time between the last observation and the moment of the identification of the sunspot groups is changed in (A1) from  $T = 17$  used for the real identification to values from 7 to 10 days characterizing the training set.

There are two types of the errors. Type I errors are false positive identifications ( $fp$  is their number), i.e., the groups identified as recurrent, whereas they are not. Type II errors are false negatives ( $fn$ ) which misidentify recurrent groups. If the number of the correct identifications of the recurrent groups is  $tp$ , then the positive prediction value  $PPV$  and the true predictive rate  $TPR$  are

$$PPV = \frac{tp}{tp + fp}, \quad TPR = \frac{tp}{tp + fn}.$$

The training is designed to maximize the score

$$F_1 = 2 \frac{PPV \cdot TPR}{PPV + TPR} = \frac{tp}{tp + 0.5(fp + fn)}$$

adjusting the semi-axes  $l_x$  and  $l_y$  of the ellipse along the longitudes and latitudes. The identification is performed with Rules 1, 1', and 2.

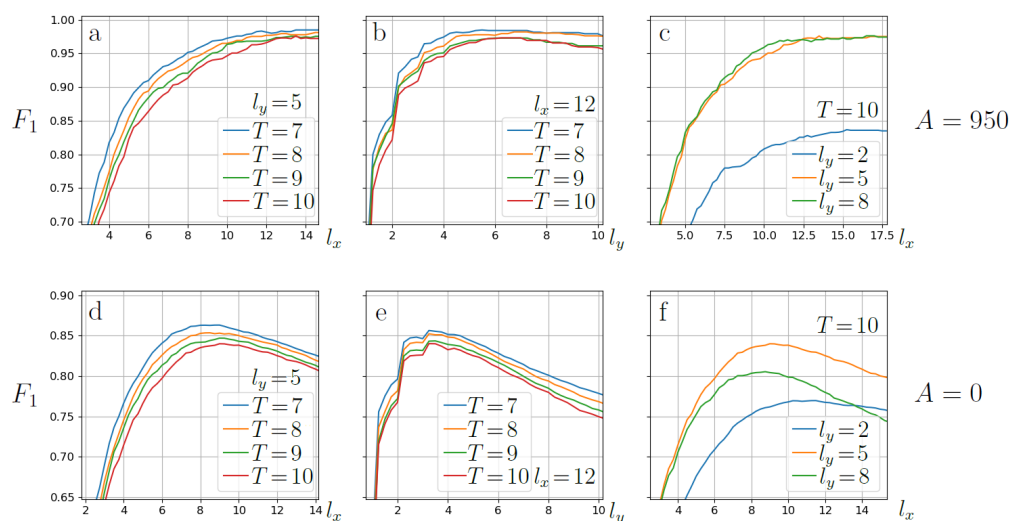


**Figure A1.** Training: The  $F_1$  score calculated on sunspot groups from the training set  $\Omega_{A,T}$  with the low threshold  $A$  of the maximal area, the variable time gap  $T$  between the observations and the longitudinal and latitudinal semi-axes of the ellipse  $l_x$  and  $l_y$ , respectively. Upper row is corresponding to  $A = 950$ , lower – to  $A = 0$ .

The values of  $l_x$  and  $l_y$  are adjusted separately for each  $A$ . The parameter  $A$  affects the choice of  $l_x$  and  $l_y$ : in general, larger values of  $A$  result in a broader ellipse. The observation agrees with the conclusions of Hathaway [10] that, in particular, cover more distant passages of larger groups. The increase-ellipse strategy can potentially catch the groups which move substantially across the Sun (in the Carrington coordinates) but is threatened by the necessity to distinguish between several groups appearing in the large ellipse. Identifying large recurrent groups, we reduce the number of the false identifications by looking for the complements with relatively large areas (Rule 1').

A general dependence of the ellipse on  $A$  is not described here. However, the adjusted values of the axes of the ellipse are almost the same for the moderate and large sunspot groups. Aggregating the best parameters over different choices of  $T$  and  $A$ , we pick up  $(l_x, l_y) = (12^\circ, 5^\circ)$  for both values of  $A$ : 950 and 700 MH (chosen to define the large and moderate recurrent groups in the main text). According to Figure A1a, if  $l_y$  is fixed to  $5^\circ$ , the score increases up to  $l_x \approx 10^\circ$ – $12^\circ$ , attains the maximum, and, eventually, saturates. Approximately the same behavior of  $l_x$  is observed for  $l_y \in [2^\circ, 5^\circ]$  (but we skip the graphs). Figure A1b illustrates the choice of  $l_y$  as the local maximum of the graphs. In general, the curves observed with different values of  $T$  agree with one another (Figure A1a,b). Then we argue that the choice of the parameters performed with  $T$  corresponding to 8–10 days is likely to be adequate for  $T = 17$  days as required for the real identification.

Interestingly, the typical shift of the sunspots along the Sun is known to be small [10]. This suggests the choice of a narrower ellipse. For example, the choice of  $l_y = 2^\circ$  corresponds to that in  $1.9^\circ$  in the paper by Nagovitsyn et al. [7]. Nevertheless, fixing this narrower  $2^\circ \times 12^\circ$  ellipse, one ends up with a smaller score (Figure A1c). Nagovitsyn et al. [7], intending to identify *all* recurrent groups, used the relatively small  $l_y \approx 2^\circ$ .

This result is confirmed by Figure A1d–f. One can see that maximal value of  $F_1$  score is approximately 0.85, whereas the maximal score for  $A = 950$  is more than 0.95. Moreover, the monotonicity of these functions is completely different. Figure A1d shows that for  $l_y = 5^\circ$  the maximal values of  $F_1$  score is observed as  $l_x \in [8^\circ, 10^\circ]$ . According to Figure A1e, if  $l_x$  is fixed to  $12^\circ$ ,  $F_1$  saturates at  $l_y = 2^\circ$  and rapidly decreases when  $l_y > 4^\circ$ . Finally, Figure A1f shows that if  $A = 0$ , the curves disagree with one another. This indicates that the increment of  $l_x$  and  $l_y$  tends to errors.

Aiming at *large* recurrent sunspot groups, we fix the larger  $l_y = 5^\circ$  as the training suggests. Further changing of  $l_y$  from  $5^\circ$  upward affects the score weakly, and we stop at  $l_y = 5^\circ$ , taking into account the evidence of small shifts known for the majority of the spots. We compare the identifications of the large recurrent groups with the value  $l_y$  fixed to  $5^\circ$  and  $2^\circ$  in more details (and  $l_x = 10^\circ$ ). There are two types of the errors during identification. Clearly, a growth in  $l_y$  reduces the number of the type II ( $fn$ ) errors at the expense of an increase in the number of the type I ( $fp$ ) errors. The Table A1 justifies that the reduction of the type II errors is reliable if  $l_y$  is switched from  $2^\circ$  to  $5^\circ$  as it is shown in Figure A1. To be precise, we increase the number of uncertain complements from  $\sim 25$  to  $\sim 125$  out of 968 and find the complement in the wider ellipse 34 times when the complement in the narrower ellipse is absent. Matching the area of the source and the complements, one reduces the number of wrong identifications as it follows from the analysis of the training set (the identification score is increased by 10%).

**Table A1.** The number of the type I and II errors for large ( $A > 950$  MH) and moderate ( $A > 700$  MH) recurrent groups;  $T = 10$ .

$A > 950$ MH	Ellipse Size $12^\circ \times 2^\circ$	Ellipse Size $12^\circ \times 5^\circ$	Number of the Groups in the Training Set
Error type I ( $fp$ )	14	8	529
Error type II ( $fn$ )	148	27	
$A > 700$ MH	$12^\circ \times 2^\circ$	$12^\circ \times 5^\circ$	Number of the groups in the training set
Error type I ( $fp$ )	26	22	920
Error type II ( $fn$ )	238	43	

**Table A2.** The errors in the identification of large sunspot groups with the ellipses of the sizes  $12^\circ \times 2^\circ$  (roughly corresponding to [7]) and  $12^\circ \times 5^\circ$  used in this paper on the training set (A3) defined with the 1944–1976 RGO/SOON catalogues and  $T = 10$ . The RGO/SOON ID are given; the pairs of the ID show the two groups that are erroneously united into a single group.

$A > 950$ MH	$12^\circ \times 2^\circ$	$12^\circ \times 5^\circ$
Error type I	(18872, 18882), (18959, 18971)	(19061, 19062),
Error type II	18559, 21356, 19200, 21506 14838, 16486, 18756, 20125, 23119 14717, 15638, 17161, 17782	17782, 18756

### Appendix C. Comparison with Other Identifications

We also compare our identification with that performed by Henwood et al. [19] and RGO, presented by [18] who processed GPR(linked) and RGO catalogues, respectively. Following Henwood et al. [19], we choose 1896 for the comparison. Then RGO and GPR(linked) are characterized by 26 and, respectively, 28 sunspot groups identified as recurrent by Maunder [18] or Henwood et al. [19]; 15 groups are common. Since our algorithm identifies large and moderate long-lived groups, we examine here only those groups that shown up the area being larger than 700 MH at least once. There are 8 such sunspot groups suggested to be recurrent by Maunder [18] or Henwood et al. [19]. Here is the list:

- (1) The matching of the groups with ID 4285–4296 presented in RGO and GPR(linked) is also with our catalogue L;
- (2) 4369–4386 is presented in GPR(linked) and M;
- (3) 4376–4399 presented in RGO and M is replaced by the matching 4376–4395 in GPR(linked);
- (4) 4416–4435–4448 in GPR(linked) corresponding to 4416–4435–4446 in RGO is identified as 4435–4447 in M (Rule 4 violated);
- (5) 4428–4441 is presented in GPR(linked) and L;
- (6) 4456–4473 is presented in RGO, GPR(linked), and M (note that GPR(linked) contains the matching 4457–4473 in addition).

There are two other matching 4256–4278 and 4295–4314 with both RGO and GPR(linked) catalogues. In these cases, the area of the source groups was larger than 950 MH but the area of the complement is smaller than 100 MH. That is, these matching pairs violate our identification Rule 1'. We conclude that our identification of the recurrent groups nicely correspond to the expert identification performed by Maunder [18] and Henwood et al. [19].

### Appendix D. Example of Potentially Wrong Identification

Figure A2 gives an example of a confusing identification: groups 11277 (the nearest) and 11279 (selected by our algorithm) appear near the location where group 11263 was previously detected. The usage of the STEREO observations suggests that this identification is wrong but leaves a room for some concerns. We recall that the goal of the identification is to quantify the role of the strong magnetic field associated with large nestlets through the composites built on the 11 or 22-year averages of the identified groups. The error in this particular identification affects the composite weakly, as both potential complements are not characterized by a large discrepancy in their areas. Even if both complements were incorrect (i.e., group 11263 vanishes at the back side of the Sun, which is unlikely) the appearance of a new large group at approximately the same location may be caused by the strong magnetic field we are going to characterize. Therefore, the inclusion of any of these groups into the composite is likely to be relevant.

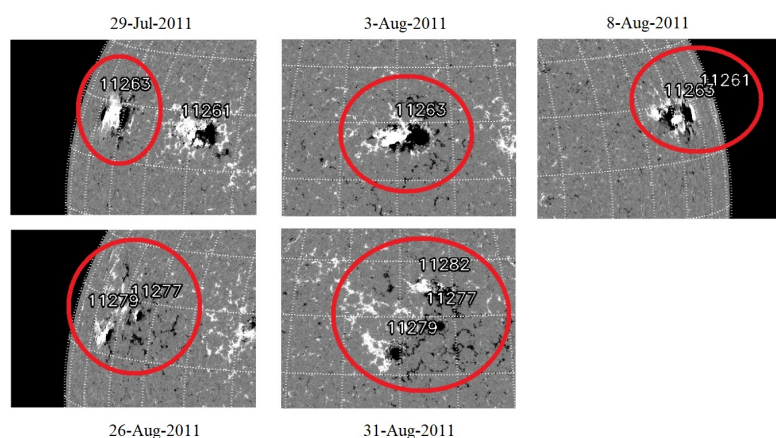


**Figure A2.** The movement of the sunspot group 11263–11277/11279 (recorded from 29 July 2011 till 4 September 2011) supposed to be recurrent. Data are freely downloaded from [SolarMonitor.org](https://solarmonitor.org) (accessed on 5 January 2022).

### References

- Rieutord, M.; Rincon, F. The Sun's supergranulation. *Living Rev. Sol. Phys.* **2010**, *7*, 1–82. [[CrossRef](#)]
- Obridko, V.; Badalyan, O. Cyclic and secular variations sunspot groups with various scales. *Astron. Rep.* **2014**, *58*, 936–944. [[CrossRef](#)]
- Mandal, S.; Banerjee, D. Sunspot sizes and the solar cycle: Analysis using Kodaikanal white-light digitized data. *Astrophys. J. Lett.* **2016**, *830*, L33. [[CrossRef](#)]
- Javaraiah, J. North-south asymmetry in small and large sunspot group activity and violation of even-odd solar cycle rule. *Astrophys. Space Sci.* **2016**, *361*, 208. [[CrossRef](#)]
- Usoskin, I.G.; Kovaltsov, G.A.; Chatzistergos, T. Dependence of the Sunspot-group size on the level of solar activity and its influence on the calibration of solar observers. *Sol. Phys.* **2016**, *291*, 3793–3805. [[CrossRef](#)]
- Osipova, A.; Nagovitsyn, Y. The Waldmeier effect for two sunspot populations. *Geomagn. Aeron.* **2017**, *57*, 1092–1100. [[CrossRef](#)]
- Nagovitsyn, Y.; Ivanov, V.; Skorbezh, N. Refinement of the Gnevyshev-Waldmeier Rule Based on a 140-Year Series of Observations. *Astron. Lett.* **2019**, *45*, 396–401. [[CrossRef](#)]
- Bazilevskaya, G.; Broomhall, A.M.; Elsworth, Y.; Nakariakov, V. A combined analysis of the observational aspects of the quasi-biennial oscillation in solar magnetic activity. *Space Sci. Rev.* **2014**, *186*, 359–386. [[CrossRef](#)]
- Popova, E.; Yuhina, N. The quasi-biennial cycle of solar activity and dynamo theory. *Astron. Lett.* **2013**, *39*, 729–735. [[CrossRef](#)]
- Hathaway, D.H. The Solar Cycle. *Living Rev. Sol. Phys.* **2015**, *12*, 4. [[CrossRef](#)]
- Le Mouél, J.L.; Lopes, F.; Courtillot, V. Identification of Gleissberg cycles and a rising trend in a 315-year-long series of sunspot numbers. *Sol. Phys.* **2017**, *292*, 43. [[CrossRef](#)]
- Petrovay, K. Solar cycle prediction. *Living Rev. Sol. Phys.* **2020**, *17*, 1–93. [[CrossRef](#)]
- Mu noz-Jaramillo, A.; Senkpeil, R.R.; Windmueller, J.C.; Amouzou, E.C.; Longcope, D.W.; Tlatov, A.G.; Navovitsyn, Y.A.; Pevtsov, A.A.; Chapman, G.A.; Cookson, A.M.; et al. Small-scale and global dynamos and the area and flux distributions of active regions, sunspot groups, and sunspots: A multi-database study. *Astrophys. J.* **2015**, *800*, 48–67. doi: [[CrossRef](#)]
- Hazra, G. Recent advances in the 3D kinematic Babcock-Leighton solar dynamo modeling. *arXiv* **2020**, arXiv:2009.03810.

15. Yeates, A.; Mu noz-Jaramillo, A. Kinematic active region formation in a three-dimensional solar dynamo model. *Mon. Not. R. Astron. Soc.* **2013**, *436*, 3366–3379. [[CrossRef](#)]
16. Miesch, M.S.; Dikpati, M. A three-dimensional Babcock-Leighton solar dynamo model. *Astrophys. J. Lett.* **2014**, *785*, L8. [[CrossRef](#)]
17. Karak, B.B.; Miesch, M. Recovery from Maunder-like grand minima in a Babcock–Leighton solar dynamo model. *Astrophys. J. Lett.* **2018**, *860*, L26. [[CrossRef](#)]
18. Maunder, A. Catalogue of Recurrent Groups of Sun Spots for the Years 1874 to 1906 Compiled by Mrs. Annie SD Maunder, from the Ledgers of Groups of Sun Spots Published in the Greenwich Observations, 1886–1907. *Greenwich Obs. Astron. Magn. Meteorol. Made R. Obs. Ser.* **1909**, *69*, O1–O50.
19. Henwood, R.; Chapman, S.; Willis, D. Increasing lifetime of recurrent sunspot groups within the Greenwich photoheliographic results. *Sol. Phys.* **2010**, *262*, 299–313. [[CrossRef](#)]
20. Ringnes, T. Secular variations of long-lived sunspots. *Astrophys. Nor.* **1964**, *8*, 303.
21. Foukal, P. An Explanation of the Differences Between the Sunspot Area Scales of the Royal Greenwich and Mt. Wilson Observatories, and the SOON Program. *Sol. Phys.* **2014**, *289*, 1517–1529. [[CrossRef](#)]
22. Giersch, O.; Kennewell, J.; Lynch, M. Reanalysis of Solar Observing Optical Network Sunspot Areas. *Sol. Phys.* **2018**, *293*, 17. [[CrossRef](#)]
23. Hathaway, D. USAF/NOAA Sunspot Data; 1875–2020. Available online: <http://solarcyclescience.com/activeregions.html> (accessed on 5 January 2022).
24. Hathaway, D.; Wilson, R.; Reichmann, E. Group Sunspot Numbers: Sunspot Cycle Characteristics. *Sol. Phys.* **2002**, *211*, 357–370. [[CrossRef](#)]
25. Balmaceda, L.; Solanki, S.; Krivova, N.; Foster, S. A homogeneous database of sunspot areas covering more than 130 years. *J. Geophys. Res. Space Phys.* **2009**, *114*, A7. [[CrossRef](#)]
26. Lockwood, M.; Owens, M.; Barnard, L.; Usoskin, I. An Assessment of Sunspot Number Data Composites over 1845–2014. *Astrophys. J.* **2016**, *824*, 54–70. [[CrossRef](#)]
27. Mandal, S.; Krivova, N.A.; Solanki, S.K.; Sinha, N.; Banerjee, D. Sunspot area catalogue revisited: Daily cross-calibrated areas since 1874. *Astrophys. J.* **2020**, *640*, A78.
28. Willis, D.; Wild, M.; Appleby, G.; Macdonald, L. The Greenwich Photo-heliographic Results (1874–1885): Observing Telescopes, Photographic Processes, and Solar Images. *Sol. Phys.* **2016**, *291*, 2553–2586. [[CrossRef](#)]
29. Cliver, E. Sunspot number recalibration: The ~1840–1920 anomaly in the observer normalization factors of the group sunspot number. *J. Space Weather Space Clim.* **2017**, *7*, A12. [[CrossRef](#)]
30. Clette, F.; Svalgaard, L.; Vaquero, J.M.; Cliver, E.W. Revisiting the sunspot number. In *The Solar Activity Cycle*; Springer: Berlin/Heidelberg, Germany, 2015; pp. 35–103.
31. Hoyt, D.V.; Schatten, K.H. Group sunspot numbers: A new solar activity reconstruction. *Sol. Phys.* **1998**, *179*, 189–219. [[CrossRef](#)]
32. Lockwood, M.; Owens, M.; Barnard, L. Centennial variations in sunspot number, open solar flux, and streamer belt width: 1. Correction of the sunspot number record since 1874. *J. Geophys. Res. Space Phys.* **2014**, *119*, 5172–5182. [[CrossRef](#)]
33. Svalgaard, L.; Schatten, K.H. Reconstruction of the sunspot group number: The backbone method. *Sol. Phys.* **2016**, *291*, 2653–2684. [[CrossRef](#)]
34. Usoskin, I.G.; Kovaltsov, G.A.; Lockwood, M.; Mursula, K.; Owens, M.; Solanki, S.K. A new calibrated sunspot group series since 1749: Statistics of active day fractions. *Sol. Phys.* **2016**, *291*, 2685–2708. [[CrossRef](#)]
35. Kaiser, M.; Kucera, T.; Davila, J.; Cyr, O.; Guhathakurta, M.; Christian, E. The STEREO mission: An introduction. *Space Sci. Rev.* **2008**, *136*, 5–16. [[CrossRef](#)]
36. Pesnell, W.; Thompson, B.; Chamberlin, P. The solar dynamics observatory (SDO). In *The Solar Dynamics Observatory*; Springer: Berlin/Heidelberg, Germany, 2011; pp. 3–15.
37. Balthasar, H.; Wöhl, H. Differential rotation and meridional motions of sunspots in the years 1940–1968. *Astron. Astrophys.* **1980**, *92*, 111–116.
38. Howard, R.; Gilman, P. Meridional motions of sunspots and sunspot groups. *T Astrophys. J.* **1986**, *307*, 389–394. [[CrossRef](#)]
39. Ruždjak, D.; Ruždjak, V.; Brajša, R.; Wöhl, H. Deceleration of the rotational velocities of sunspot groups during their evolution. *Sol. Phys.* **2004**, *221*, 225–236. [[CrossRef](#)]
40. SILSO World Data Center. The International Sunspot Number. In *International Sunspot Number Monthly Bulletin and Online Catalogue*; SILSO World Data Center: Brussels, Belgium, 2020.
41. Blanter, E.; Le Mouél, J.L.; Perrier, F.; Shnirman, M. Short-term correlation of solar activity and sunspot: Evidence of lifetime increase. *Sol. Phys.* **2006**, *237*, 329–350. [[CrossRef](#)]
42. Lockwood, M.; Owens, M.; Barnard, L.; Usoskin, I. Tests of Sunspot Number Sequences: 3. Effects of Regression Procedures on the Calibration of Historic Sunspot Data. *Sol. Phys.* **2016**, *291*, 2829–2841. [[CrossRef](#)]
43. Willis, D.M.; Wild, M.N.; Warburton, J.S. Re-examination of the Daily Number of Sunspot Groups for the Royal Observatory, Greenwich (1874–1885). *Sol. Phys.* **2016**, *291*, 2519–2552. [[CrossRef](#)]
44. Javaraiah, J. The G–O rule and Waldmeier effect in the variations of the numbers of large and small sunspot groups. *Sol. Phys.* **2012**, *281*, 827–837. [[CrossRef](#)]
45. Kilcik, A.; Yurchyshyn, V.; Ozguc, A.; Rozelot, J. Solar cycle 24: Curious changes in the relative numbers of sunspot group types. *Astrophys. J. Lett.* **2014**, *794*, L2. [[CrossRef](#)]

46. Shapoval, A.; Le Mouél, J.L.; Shnirman, M.; Courtillot, V. Observational evidence in favor of scale-free evolution of sunspot groups. *Astron. Astrophys.* **2018**, *618*, A183. [[CrossRef](#)]
47. Castenmiller, M.; Zwaan, C.; van der Zalm, E.B.J. Sunspot nests. *Sol. Phys.* **1986**, *105*, 237. [[CrossRef](#)]
48. Petrie, G. Solar Magnetism in the Polar Regions. *Living Rev. Sol. Phys.* **2015**, *12*, 1–102. [[CrossRef](#)]
49. Ugarte-Urra, I.; Upton, L.; Warren, H.; Hathaway, D. Magnetic flux transport and the long-term evolution of solar active regions. *Astrophys. J.* **2015**, *815*, 90. [[CrossRef](#)]
50. Gyenge, N.; Singh, T.; Kiss, T.; Srivastava, A.; Erdélyi, R. Active Longitude and Coronal Mass Ejection Occurrences. *Astrophys. J.* **2017**, *838*, 18. [[CrossRef](#)]
51. Thompson, W. Coordinate systems for solar image data. *Astron. Astrophys.* **2006**, *449*, 791–803. [[CrossRef](#)]
52. Petrovay, K.; van Driel-Gesztelyi, L. Making sense of sunspot decay—I: Parabolic Decay Law and Gnevyshev–Waldmeier Relation. *Sol. Phys.* **1997**, *176*, 249–266. [[CrossRef](#)]